Available online at www.sciencedirect.com
ScienceDirect
Journal of Solid State Chemistry 180 (2007) 106–112
JOURNAL OF SOLID STATE CHEMISTRY
www.elsevier.com/locate/jssc

# The role of cation–cation interactions in a neptunyl chloride hydrate and topological aspects of neptunyl structural units

T.Z. Forbes, P.C. Burns*

*Department of Civil Engineering and Geological Sciences, University of Notre Dame, 156 Fitzpatrick Hall, Notre Dame, IN 46656, USA*

Received 20 July 2006; received in revised form 29 September 2006; accepted 30 September 2006
Available online 6 October 2006

**Abstract**

The compound $K_4(NpO_2)_3Cl_7(H_2O)_4$ was synthesized by evaporation of a $Np^{5+}$-bearing solution. The crystal structure was determined by single crystal X-ray diffraction and refined to $R_1 = 0.0374$. The compound is triclinic, $P\bar{1}$, $a = 8.882(1)$ Å, $b = 12.082(2)$ Å, $c = 12.403(2)$ Å, $\alpha = 65.855(2)^\circ$, $\beta = 69.604(2)^\circ$, $\gamma = 74.432(2)^\circ$, $V = 1126.0(3)$ Å$^3$, and $Z = 2$. The structure contains dimers of edge sharing $Np^{5+}$ pentagonal bipyramids that are linked into infinite chains through cation–cation interactions with an additional $Np^{5+}$ pentagonal bipyramid. The structural units are linked through bonds to interstitial K cations and by H bonding. A graphical representation for neptunyl structural units including cation–cation interactions is introduced.


*Keywords:* Neptunium; Structure determination; X-ray diffraction; Cation–cation interactions; Graphical representation

## 1. Introduction

The coordination chemistry of hexavalent and pentavalent actinides is complex [1,2]. The crystal chemistry of $U^{6+}$ has been extensively investigated, in part because of its occurrence in nature and importance in the nuclear fuel cycle [3–5]. $U^{6+}$ usually forms a nearly linear dioxo uranyl cation, $(UO_2)^{2+}$, with $U^{6+}$–O bond lengths of 1.79(4) Å, corresponding to strong covalent bonds [6,7]. Additional bonding is required to satisfy the remaining valence of the uranyl ion, and typically four, five, or six ligands are arranged at the equatorial vertices of square, pentagonal, and hexagonal bipyramids [6]. Bonding to the $U^{6+}$ cation alone satisfies most of the requirements of the uranyl ion oxygen atoms ($O_{Ur}$), but the equatorial ligands require additional linkages. Most linkages of uranyl polyhedra to other polyhedra containing higher valence cations takes place through the equatorial vertices, most often resulting in the formation of infinite chains or sheets [7].

Much less is known about the structures of $Np^{5+}$ compounds, but the few structures that have been described exhibit similar coordination about $Np^{5+}$ as observed for $U^{6+}$. $Np^{5+}$ occurs as a dioxo cation, although the bond distances are slightly longer at 1.83 Å [1]. The neptunyl ion is usually coordinated by from four to six ligands arranged at the equatorial vertices of square, pentagonal, and hexagonal bipyramids. The $Np^{5+}$–O bonds within the neptunyl ion are somewhat weaker than those in uranyl ions, which permits linkages of the neptunyl polyhedra through the neptunyl ion oxygen atom (a cation–cation interaction), resulting in a divergence from the crystal chemistry of $U^{6+}$[1].

First recognized by Sullivan et al., 1961 [8], the designation ‘‘cation–cation interaction’’ describes the situation where an O atom of an actinyl ion is also an equatorial ligand of a neighboring actinyl polyhedron. This interaction has been observed in solution using a variety of techniques including absorption, vibrational, and Mossbauer spectroscopies, as well as X-ray scattering [9]. Cation–cation interactions in the solid state were first observed in 1984 when the structure of $[Na_4(NpO_2)_2(C_{12}O_{12})](H_2O)_8$ was reported, yielding a dimer of Np polyhedra featuring this interaction [10]. Currently there are approximately 30 inorganic structures known that contain $Np^{5+}$, with 11 having cation–cation interactions

*Corresponding author. Fax: +574 631 9236.
*E-mail address:* pburns@nd.edu (P.C. Burns).

0022-4596/$ - see front matter © 2006 Elsevier Inc. All rights reserved.
doi:10.1016/j.jssc.2006.09.026

linking the neptunyl polyhedra into chains, sheets, and frameworks [11–20].

We have undertaken a detailed study of $Np^{5+}$ crystal chemistry, focusing on compounds with environmentally relevant chemical compositions. This research is motivated in part by the importance of $^{237}Np$ for the geologic disposal of commercial spent nuclear fuel [21]. $^{237}Np$ has a long half-life ($2.14 \times 10^6$ years) and $Np^{5+}$ is soluble in groundwater, where it complexes with a variety of ligands, including sulfate [22]. Understanding the crystal chemistry of $Np^{5+}$ will improve our ability to predict its behavior in the solid state as well as providing a basis for studying complexation of $Np^{5+}$ in solution. Here we present the synthesis and structure of a novel $Np^{5+}$ chloride that contains chains of neptunyl polyhedra involving cation–cation interactions. We also develop a graphical representation of neptunyl structures based upon their fundamental building blocks that can be used to organize neptunium crystal structures into hierarchical sequences and to identify structural trends within a larger group of compounds that contain a variety of chemical species.

## 2. Experimental methods

### 2.1. Crystal synthesis

The reagents KCl (Fisher Scientific Lot # 783390) and $NH_4OH$ (J.T. Baker Lot #30960) were used as received. A stock solution of $(NpO_2)^+$ was prepared by purification using a cation-exchange column containing Dowex-50-X8 resin. The Np was dissolved in a 1 M HCl solution to a concentration of 98 mmol $Np^{5+}$. UV spectroscopy was used to verify that the solution contained $Np^{5+}$ only. *CAUTION: $^{237}Np$ represents a serious health risk due to the emission of alpha and gamma radiation. Such studies require appropriate equipment and personnel for handling radioactive materials.* KCl (0.0250 g), 0.5 mL $Np^{5+}$ stock solution, and 0.5 mL of ultra-pure water (18 MΩ) were added to a 7-mL Teflon cup with a screw-top lid. The pH was adjusted from 0.2 to 2.8 by the addition of 230 μL of concentrated $NH_4OH$. The cup was then sealed and placed into a 125 mL Parr acid digestion vessel and 50 mL of ultrapure water was added to the vessel to provide counter-pressure during heating. Heating took place in a gravity convection oven at 160 °C for six days. The vessel was allowed to cool slowly to room temperature before removal from the oven. After the heat cycle, no solids had formed and the solution retained a green color. The solution was allowed to evaporate to near dryness, which resulted in the growth of green platy crystals approximately 200 μM in diameter.

### 2.2. Structure solution and refinement

A suitable single crystal of $K_4(NpO_2)_3Cl_7(H_2O)_4$ was mounted on a glass fiber and placed on a Bruker three-circle X-ray diffractometer equipped with an APEX II CCD detector. A sphere of three-dimensional data was collected at room temperature using monochromatic Mo$K\alpha$ radiation. The counting time per frame was 20 s with frame widths of 0.3° in $\omega$. Unit cell parameters, refined by least-squares techniques, and data integration were completed using the Bruker APEX software [23]. A semi-empirical absorption correction was applied to the data by modeling the crystal as an ellipsoid using the Bruker program XPREP. Table 1 lists selected data collection parameters and crystallographic data for $K_4(NpO_2)_3Cl_7(H_2O)_4$.

The structure was solved by direct methods and refined on the basis of $F^2$ for all unique data using the Bruker APEX software [23]. Atomic scattering factors for each atom were taken from International Tables of X-ray Crystallography [24]. The Np and K cations were found in direct-methods solutions and the O and Cl atoms were located in the difference-Fourier maps calculated following refinements of the partial structure model. The structure was initially solved in space group $P1$, but an inversion center was located using the program PLATON [25] and the final model was placed in space group $P\bar{1}$. The final model includes anisotropic displacement parameters for all

Table 1
Crystal data and structure refinement for $K_4(NpO_2)_3Cl_7(H_2O)_4$

| | | | |
|---|---|---|---|
| Formula | $K_4(NpO_2)_3Cl_7(H_2O)_4$ | Crystal size (mm) | $0.15 \times 0.10 \times 0.01$ |
| Formula weight | 1283.6 | Theta range | 2.87–32.68 |
| Temperature | 293(2) K | Data collected | $-13<h<13$ |
| Crystal system | Triclinic, $P\bar{1}$ | | $-18<k<18$ |
| $a$ (Å) | 8.882(1) | | $-18<l<18$ |
| $b$ (Å) | 12.082(2) | Reflections collected | 16826 |
| $c$ (Å) | 12.403(2) | Reflections unique | 7674 |
| $\alpha$ | 65.855(2) | $R_{int}$ | 0.0587 |
| $\beta$ | 69.604(2) | Data/restraints/parameters | 7674/8/241 |
| $\gamma$ | 74.432(2) | GOF on $F^2$ | 0.814 |
| Volume (Å$^3$) | 1126.0(3) | Final $R$ indices $I>2\sigma(I)$ | $R_1 = 0.0374$, |
| $Z$ | 2 | | $wR_2 = 0.0512$ |
| $D_{calc}$ (g/cm$^3$) | 3.786 | $R$ indices (all data) | $R_1 = 0.0979$ |
| $\mu$ (mm$^{-1}$) | 15.34 | Largest diff peak and hole | 2.352 |
| $F$(000) | 1124 | (Å$^{-3}$) | −3.173 |

Table 2
Atomic coordinates ($\times 10^4$) and equivalent isotropic displacement parameters ($Å^2 \times 10^3$) for $K_4(NpO_2)_3Cl_7(H_2O)_4$

| | x | y | z | U (eq) |
|---|---|---|---|---|
| Np(1) | 4008(1) | 721(1) | 8321(1) | 15(1) |
| Np(2) | 2682(1) | 2470(1) | 4927(1) | 18(1) |
| Np(3) | 1007(1) | 4288(1) | 1695(1) | 15(1) |
| K(1) | 526(2) | 7803(2) | 1298(2) | 33(1) |
| K(2) | 5505(2) | 2825(2) | 1470(2) | 36(1) |
| K(3) | 6417(2) | 6044(2) | 1671(2) | 34(1) |
| K(4) | 1142(3) | 614(2) | 2499(3) | 56(1) |
| Cl(1) | −1237(3) | 3907(2) | 733(2) | 25(1) |
| Cl(2) | 3681(3) | −1056(2) | 747(2) | 30(1) |
| Cl(3) | 1574(3) | −519(2) | 8595(2) | 27(1) |
| Cl(4) | 3420(3) | 5593(2) | 1294(2) | 28(1) |
| Cl(5) | 1847(3) | 308(2) | 5122(2) | 34(1) |
| Cl(6) | 5522(3) | 3595(2) | 3981(2) | 31(1) |
| Cl(7) | −701(3) | 2625(3) | 6088(2) | 38(1) |
| O(1) | 2479(7) | 3197(6) | 1041(6) | 24(2) |
| O(2) | 2513(7) | 1810(6) | 8927(6) | 27(2) |
| O(3) | −513(7) | 5380(6) | 2330(6) | 26(2) |
| O(4) | 5540(7) | −368(6) | 7701(6) | 26(2) |
| O(5) | 2181(7) | 3236(6) | 3441(5) | 25(2) |
| O(6) | 5508(7) | 2547(7) | 6817(6) | 28(2) |
| O(7) | −618(7) | 2589(7) | 3347(6) | 30(2) |
| O(8) | 3182(7) | 1735(6) | 6398(6) | 32(2) |
| O(9) | 5084(7) | 1246(6) | 3891(6) | 29(1) |
| O(10) | 1860(8) | 4443(6) | 5312(6) | 39(2) |
| H(1) | 6590(50) | 2460(90) | 6870(90) | 50 |
| H(2) | −1710(50) | 2820(90) | 3790(80) | 50 |
| H(3) | 4800(120) | 490(50) | 4010(90) | 50 |
| H(4) | 990(80) | 4410(90) | 5050(90) | 50 |
| H(5) | 5260(120) | 2070(30) | 3610(90) | 50 |
| H(6) | −1640(60) | 3090(80) | 3470(100) | 50 |
| H(7) | 2800(60) | 4240(90) | 5610(90) | 50 |
| H(8) | 5430(1 1 0) | 2820(90) | 6000(40) | 50 |

Table 3
Selected bond lengths [Å] and angles [°] for $K_4(NpO_2)_3Cl_7(H_2O)_4$

| | | | |
|---|---|---|---|
| Np(1)–O(2) | 1.798(6) | K(2)–O(9) | 2.777(7) |
| Np(1)–O(4) | 1.820(6) | K(2)–O(1) | 2.803(6) |
| Np(1)–O(8) | 2.465(6) | K(2)–O(4)[e] | 3.008(7) |
| Np(1)–O(6) | 2.569(7) | K(2)–Cl(4)[f] | 3.107(3) |
| Np(1)–Cl(3) | 2.802(2) | K(2)–Cl(1)[g] | 3.183(3) |
| Np(1)–Cl(2) | 2.862(2) | K(2)–Cl(3)[e] | 3.264(3) |
| Np(1)–Cl(2)[a] | 2.862(2) | K(2)–Cl(4) | 3.320(3) |
| Np(2)–O(8) | 1.828(6) | K(3)–O(2)[h] | 2.727(7) |
| Np(2)–O(5) | 1.845(6) | K(3)–O(6)[h] | 2.855(7) |
| Np(2)–O(10) | 2.490(7) | K(3)–O(3)[g] | 2.931(6) |
| Np(2)–O(9) | 2.518(6) | K(3)–O(1)[f] | 2.962(7) |
| Np(2)–Cl(5) | 2.798(2) | K(3)–Cl(4) | 3.075(3) |
| Np(2)–Cl(7) | 2.836(2) | K(3)–Cl(1)[g] | 3.200(3) |
| Np(2)–Cl(6) | 2.839(2) | K(3)–Cl(6) | 3.215(3) |
| Np(3)–O(1) | 1.820(6) | K(4)–O(4)[e] | 2.814(6) |
| Np(3)–O(3) | 1.828(6) | K(4)–O(7) | 2.855(8) |
| Np(3)–O(5) | 2.450(6) | K(4)–Cl(3)[i] | 3.198(3) |
| Np(3)–O(7) | 2.565(7) | K(4)–Cl(5)[i] | 3.230(4) |
| Np(3)–Cl(4) | 2.786(2) | K(4)–Cl(5) | 3.380(4) |
| Np(3)–Cl(1) | 2.864(2) | K(4)–Cl(2)[j] | 3.407(4) |
| Np(3)–Cl(1)[b] | 2.881(2) | | |
| K(1)–O(2)[c] | 2.706(6) | | |
| K(1)–O(3) | 2.935(7) | | |
| K(1)–Cl(3)[d] | 3.081(3) | | |
| K(1)–Cl(7)[c] | 3.121(4) | | |
| K(1)–Cl(4) | 3.171(3) | | |
| K(1)–Cl(2)[d] | 3.192(3) | | |
| K(1)–Cl(3)[c] | 3.341(3) | | |

Symmetry transformations used to generate equivalent atoms: (a) $-x+1, -y, -z+2$; (b) $-x, -y+1, -z$; (c) $-x, -y+1, -z+1$; (d) $x, y+1, z-1$; (e) $-x+1, -y, -z+1$; (f) $-x+1, -y+1, -z$; (g) $x+1, y, z$; (h) $-x+1, -y+1, -z+1$; (i) $-x, -y, -z+1$; and (j) $x, y, z-1$.

non-H atoms. Bond-valence calculations indicated the presence of $H_2O$ groups, and H atoms were located in the difference-Fourier map and were refined with the soft constraint that O–H bonds be ~0.96 Å. The atomic positional parameters and selected interatomic distances for $K_4(NpO_2)_3Cl_7(H_2O)_4$ are in Tables 2 and 3, respectively.

## 3. Results

There are three symmetrically independent $Np^{5+}$ cations in $K_4(NpO_2)_3Cl_7(H_2O)_4$, each of which are strongly bonded to two O atoms, forming nearly linear neptunyl $(NpO_2)^+$ ions. The bond lengths of the neptunyl ions range from 1.798(6) to 1.845(6) Å, consistent with $Np^{5+}$. The neptunyl ions are each further coordinated by two O or $H_2O$ and three Cl atoms that are arranged at the equatorial vertices of pentagonal bipyramids that are capped by the neptunyl ion O atoms. The $Np–O_{eq}$ (eq: equatorial) bond lengths range from 2.450(6) to 2.569(7) Å, and the $Np–Cl_{eq}$ bond lengths are longer at 2.786(2) to 2.881(2) Å.

Two symmetrically identical Np(1) pentagonal bipyramids share the Cl(2)–Cl(2) edge, giving a dimer (Fig. 1). Likewise, two Np(3) bipyramids form a dimer by sharing their Cl(1)–Cl(1) edge. The dimers of Np(1) and Np(3) polyhedra are linked through the Np(2) neptunyl ion via cation–cation interactions. Specifically, both of the O atoms of the Np(2) neptunyl ion participate in cation–cation interactions, one with a Np(1) dimer and the other with the Np(3) dimer. The unshared ligands along the edges of the chain either correspond to neptunyl ion O atoms of Np(1) and Np(3), or are Cl anions or $H_2O$ groups.

Two of the equatorial vertices of the Np(2) bipyramid correspond to $H_2O$ groups, whereas the Np(1) and Np(2) polyhedra each contain one $H_2O$ group. The O(6) $H_2O$ group is bonded to Np(1), and H bonds extend to chlorine acceptors [Cl(7) and Cl(6)] on a neighboring chain of neptunyl polyhedra. The acceptor lengths are 2.29 Å for H(1)–Cl(7) and 2.26 Å for H(8)–Cl(6). The O(9) and O(10) $H_2O$ groups are bonded to Np(2) and the H bonds for O(9) extend to chlorine acceptors [Cl(5) and Cl(6)] while the H bonds for O(10) extend to the chlorine atoms [Cl(6) and Cl(7)] of the neighboring chain. The acceptor lengths are 2.56 Å for H(3)–Cl(5), 2.59 Å for H(4)–Cl(7), 2.13 Å for H(5)–Cl(6), and 2.71 Å for H(7)–Cl(6). The Np(3)

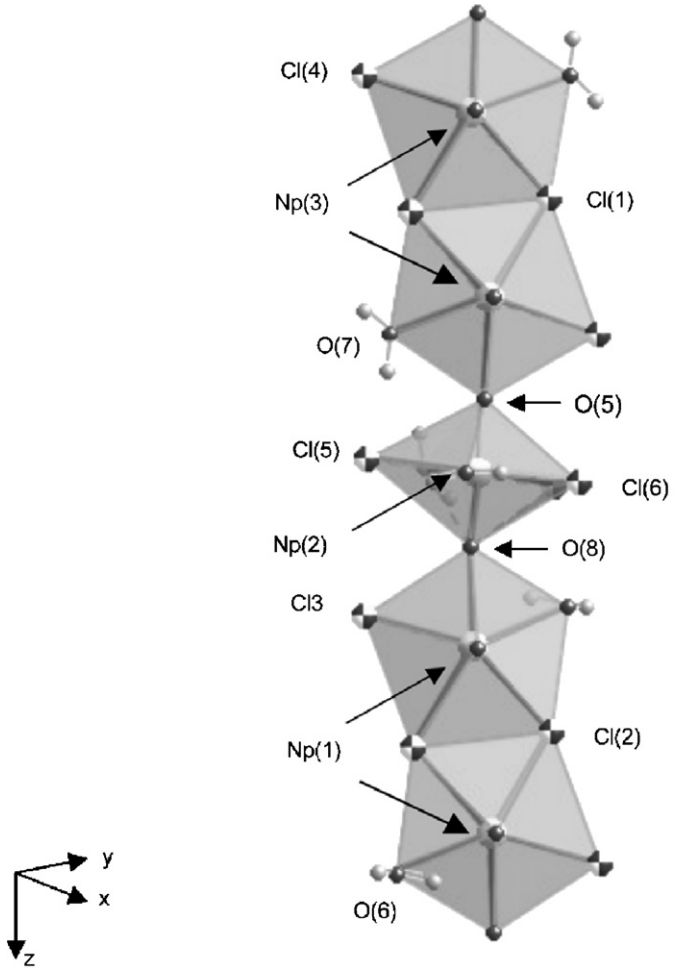


Fig. 1. Dimers of neptunyl pentagonal bipyramids in $K_4(NpO_2)_3Cl_7(H_2O)_4$ linked into chains through cation–cation interactions. Cl atoms are shown as two-toned spheres and O atoms and $H_2O$ groups are shown as solid spheres.

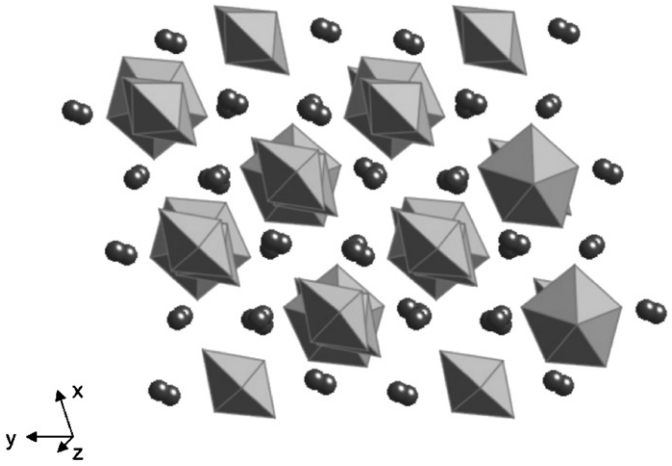


Fig. 2. Four symmetrically independent K atoms (spheres) are located between the infinite chains of neptunyl polyhedra in $K_4(NpO_2)_3Cl_7(H_2O)_4$.

polyhedron contains one $H_2O$ ligand [O(7)]. The H bonds from O(7) extend to chlorine acceptors [Cl(6)] on the neighboring chains. The acceptor lengths are 2.65 Å for H(2)–Cl(6) and 2.35 Å H(6)–Cl(6).

The chains of neptunyl polyhedra extend along [001] and are linked through bonds to four symmetrically independent K cations (Fig. 2). The K(1), K(2), and K(4) cations are coordinated by seven ligands (O and Cl atoms), and K(3) is coordinated by six ligands. The distances of K–O bonds range from 2.706(6) to 3.008(7) Å, and the K–Cl bonds are longer at 3.075(3) to 3.341(3) Å.

### 3.1. Graphical representation of neptunyl structural units

Building a graphical (or nodal) representation of the structural units within groups of compounds permits the description of complex structural topologies and the discovery of relationships between compounds with different chemistry [26]. This approach has been used extensively for inorganic compounds and minerals including the description of complex zeolites [27] and aluminophophates [28,29], as well as borate [30], sulfate [31], phosphate [32], and uranyl oxysalts [2].

The graph of a structure contains nodes that represent different types of cation-centered polyhedra. Different colors are used to represent geometrically and/or chemically distinct polyhedra. Graphical representations of uranyl compounds typically use black nodes to represent $U^{6+}$ polyhedra and white nodes to represent the cations with lower coordination geometries such as molybdate or sulfate tetrahedra [2,26]. Nodes are connected by lines where their corresponding polyhedra share at least one vertex. Single connector lines denote the sharing of one vertex between two polyhedra, double connector lines represent bidentate coordination (edge sharing), and three connector lines indicate face sharing between the polyhedra.

Graph theory can be extended to represent a hierarchy of structural units that correspond to the polymerization of higher-valence coordination polyhedra [33,34]. This hierarchical approach has been extensively applied to inorganic compounds and mineral species [2,7,31,32,35–38]. Such structural hierarchies organize complex structures into a cohesive framework that facilitates recognition of structural trends. As an example, Krivovichev [26] showed that the sheets found in a variety of uranyl compounds containing tetrahedrally coordinated hexavalent cations are mostly derived from a single parent graph by the simple deletion of nodes and connectors.

Extension of the approach for uranyl compounds [26] to $Np^{5+}$ compounds will facilitate development of a structural hierarchy that can account for the unusual properties of these structures. Burns [2], extended an earlier hierarchy of $U^{6+}$ compounds, and included graphical representations of complex chains and sheets that are dominated by vertex sharing.

Here we adopt a similar approach for $Np^{5+}$ structures, with $Np^{5+}$ polyhedra represented by black nodes. Cation–cation interactions within $Np^{5+}$ structures cause

divergence from $U^{6+}$ structures and require special attention. Cation–cation linkages are designated in the graph by an arrowhead pointing from the node that corresponds to the donating neptunyl ion. Two neptunyl ions participate in any given cation–cation interaction. In the case of the shared O atom, it is double bonded to one $Np^{5+}$ cation (the donor atom) with a bond-length of approximately 1.8 Å, and is single bonded to the second $Np^{5+}$ cation (the acceptor) with a bond length of approximately 2.4 Å. Given that any neptunyl ion can donate at most two cation–cation interactions, no more than two arrows may originate at any node in the graph. In principle, a neptunyl ion can accept as many cation–cation interactions as it has equatorial vertices, thus nodes in the graph may have zero to six incoming arrows. This approach presents a clear indication of the orientation of the cation–cation interactions between neptunyl polyhedra, as well as their frequency within the graph. The polyhedral and graphical representations for the chain in $K_4(NpO_2)_3Cl_7(H_2O)_4$ are shown in Fig. 3a and 3b, respectively. Both of the $O_{Np}$ in the Np(2) polyhedra are involved in cation–cation interactions as shown by two arrowheads originating at the corresponding black node (Fig. 3b).

Several neptunyl chloride compounds contain isolated clusters and chain structural units. $Cs_3(NpO_2)Cl_4$ contains isolated neptunyl square bipyamids with Cl atoms located at the equatorial vertices [39,40]. Cs atoms are positioned between each of the neptunyl polyhedra.

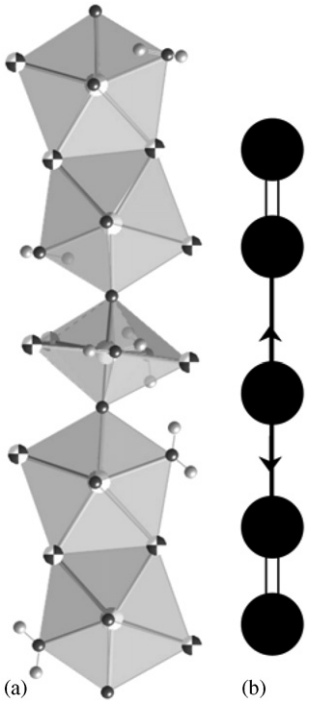


Fig. 3. The infinite chain found in $K_4(NpO_2)_3Cl_7(H_2O)_4$ (a) and its graphical representation (b) with black circles representing the neptunyl polyhedra. The cation–cation interactions are represented by single lines with arrowheads pointing from the node that corresponds to the donor neptunyl ion.

The $Np^{5+}$ cation in the structure of $Cs(NpO_2)Cl_2(H_2O)$ is in pentagonal bipyramidal coordination with four Cl atoms and one $H_2O$ group located at the equatorial vertices (Fig. 4) [40]. The pentagonal bipyramids share Cl–Cl edges, forming a chain that is one polyhedra wide that does not incorporate cation–cation interactions (Fig. 4). The structures of moctezumite ($PbTe[(UO_2)O_3]$) [41] and $[(UO_2)Cl_2H_2O]$ [42] contain topologically identical chains of pentagonal bipyramids. The equatorial ligands in the uranyl polyhedra in $[(UO_2)Cl_2H_2O]$ include four Cl atoms, with one $H_2O$ group located at the unshared vertex. The uranyl peroxide mineral studtite ($[(UO_2)(O_2)(H_2O)_2](H_2O)_2$) contains a chain with the same graphical representation [43], but with uranyl hexagonal bipyramids. Peroxide groups are the shared edges of the bipyramids in the structure of studtite.

Infinite chains of neptunyl polyhedra containing cation–cation interactions occur in $(NpO_2)(ClO_4)(H_2O)_{417}$ and $(NpO_2)_2(NO_3)_2(H_2O)_5$ [11]. The one symmetrically

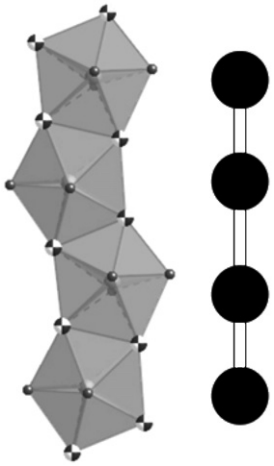

Fig. 4. $Cs(NpO_2)Cl_2(H_2O)$ [40] contains infinite chains of pentagonal bipyramids with no cation–cation interactions. The graphical representation is shown with the black circles representing neptunyl polyhedra.

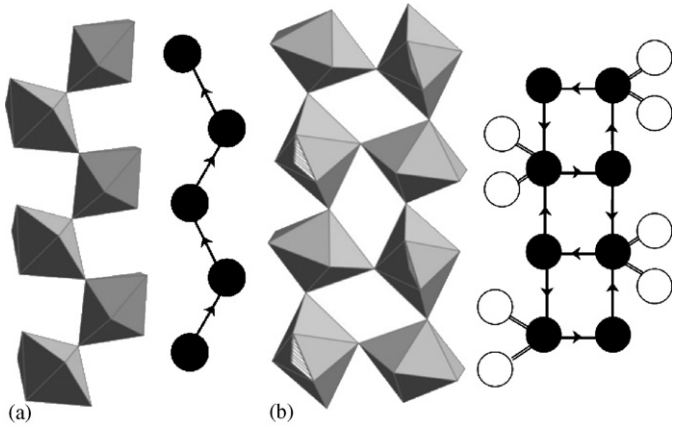


Fig. 5. Infinite chains with cation–cation interactions in (a) $(NpO_2)(ClO_4)(H_2O)_{417}$ and (b) $(NpO_2)_2(NO_3)_2(H_2O)_5$ [11]. Arrowheads point from the node that correspond to the donor neptunyl ion. The white spheres in (b) represent nitrate triangles.

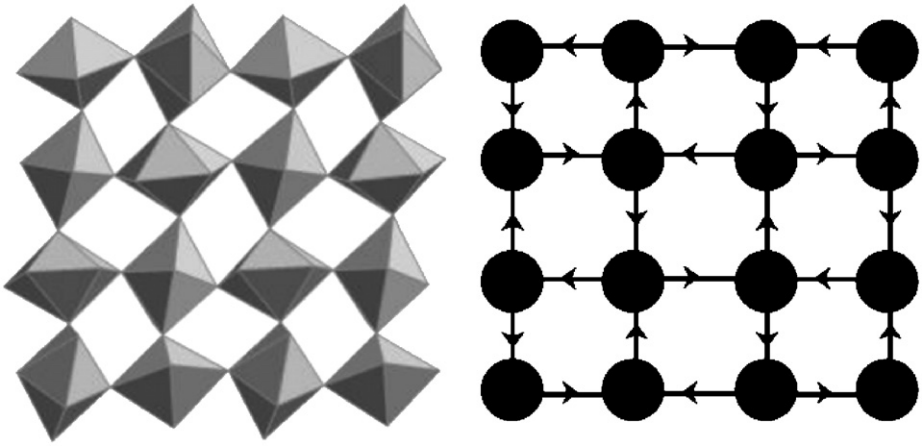

Fig. 6. $(NpO_2)Cl(H_2O)$ [44] is composed of sheets of neptunyl pentagonal bipyramids with cation–cation interactions. The nodal representation is shown with the black circles representing neptunyl polyhedra.

independent $Np^{5+}$ cation in $(NpO_2)(ClO_4)(H_2O)_4$ occurs in a pentagonal bipyramidal geometry (Fig. 5a) [17]. Four of the equatorial vertices of the pentagonal bipyramid correspond to $H_2O$. The perchlorate tetrahedra are between the chains and are connected to them by H bonds. Only one of the $O_{Np}$ atoms of each of nepunyl ion donate cation–cation interactions (Fig. 5a) $(NpO_2)_2(NO_3)_2(H_2O)_5$ contains chains of neptunyl pentagonal and hexagonal bipyramids (Fig. 5b) [11]. The neptunyl ion of the pentagonal bipyramid donates two cation–cation interactions that are accepted by the neighboring hexagonal bipyramids. The hexagonal bipyramids then donate one cation–cation interaction that is accepted by pentagonal bipyramids on a neighboring chain. This creates a chain of pentagonal and hexagonal bipyramids that is two neptunyl polyhedra wide. In addition, two nitrate triangles are found in bidentate coordination to the hexagonal bipyramid.

The sheet of polyhedra in $(NpO_2)Cl(H_2O)$ contains cation–cation interactions that link the neptunyl pentagonal bipyramids (Fig. 6) [44]. The sheet contains two symmetrically independent $Np^{5+}$ cations and both neptunyl ions donate two cation–cation interactions. The equatorial vertices that do not accept cation–cation interactions contain $H_2O$ groups or Cl atoms. The same sheet topology is also found in the structures of $[(NpO_2)_2(SO4)(H_2O)_2]$ [20], $[(NpO_2)HCOO(H_2O)]$ [45], $[(NpO_2)(C_6H_5COO)(H_2O)](H_2O)_{0.75}$ [46], $[(NpO_2)_2CH_3(COO)_2(H_2O)_2]H_2O]$ [47], and $(NpO_2)_2\{o\text{-}C_6H_5(COO)_2\}H_2O)_3](H_2O)$ [48].

## Acknowledgments

We thank Dr. L. Soderholm and Dr. S. Skanthakumar of Argonne National Laboratory for assistance. This research was funded by the National Science Foundation Environmental Molecular Science Institute at the University of Notre Dame (EAR02-21966).

## References

[1] P.C. Burns, R.C. Ewing, M.L. Miller, J. Nucl. Mater. 245 (1997) 1–9.
[2] P.C. Burns, Can. Miner. 43 (2005) 1839–1894.
[3] K.A. Hughes Kubatko, K.B. Helean, A. Navrotsky, P.C. Burns, Science 302 (2003) 1191–1193.
[4] P.C. Burns, K.M. Deely, S. Skanthakumar, Radiochim. Acta 92 (2004) 151–159.
[5] P.A. Finn, R. Finch, E. Buck, J. Bates, Mater. Res. Soc. Symp. 506 (1998) 123–131.
[6] P.C. Burns, R.C. Ewing, F.C. Hawthorne, Can. Miner. 35 (1997) 1551–1570.
[7] P.C. Burns, Rev. Miner. 38 (1999) 23–90.
[8] J.C. Sullivan, J.C. Hindman, A.J. Zielen, J. Am. Chem. Soc. 83 (1961) 3373–3378.
[9] T. Albrecht-Schmitt, P.M. Almond, R. Sykora, Inorg. Chem. 42 (2003) 3788–3795.
[10] A. Cousson, S. Dabos, H. Abazli, F. Nectoux, M. Pages, G.J. Choppin, J. Less-Common Metals 99 (1984) 233–240.
[11] M.S. Grigor'ev, I.A. Charushnikova, N.N. Krot, A.I. Yanovskii, Y.T. Struchkov, Zh. Neor. Khim. 39 (1994) 179–183.
[12] N.N. Krot, M.S. Grigoriev, Rus. Chem. Rev. 73 (2004) 89–100.
[13] T.Z. Forbes, P.C. Burns, J. Solid State Chem. 178 (2005) 3445–3452.
[14] T.Z. Forbes, P.C. Burns, Am. Miner. 91 (2006) 1089–1093.
[15] T.Z. Forbes, P.C. Burns, L. Soderholm, S. Skanthakumar, Chem. Mater. 18 (2006) 1643–1649.
[16] T.Z. Forbes, P.C. Burns, L. Soderholm, S. Skanthakumar (2006). in preparation.
[17] M.S. Grigor'ev, N.A. Baturin, A.A. Bessonov, N.N. Krot, Radiokhimiya 37 (1995) 15–18.
[18] M.S. Grigor'ev, A.M. Fedoseev, N.A. Budantseva, A.I. Yanovskii, Y.T. Struchkov, N.N. Krot, Radiokhimiya 33 (1991) 54–61.
[19] M.S. Grigor'ev, A.I. Yanovskii, A.M. Fedoseev, N.A. Budantseva, Y.T. Struchkov, N.N. Krot, Radiokhimiya 33 (1991) 17–19.
[20] M.S. Grigor'ev, A.I. Yanovskii, A.M. Fedoseev, N.A. Budantseva, Y.T. Struchkov, N.N. Krot, V.I. Spitsyn, Dokl. Akad. Nauk. 300 (1988) 618–622.
[21] R.J. Silva, H. Nitsche, Radiochim. Acta 70/71 (1995) 377–396.
[22] K.H. Lieser, U. Muhlenweg, Radiochim. Acta 43 (1988) 27–35.
[23] Bruker, Madison, WI, 2005.
[24] J.A. Ibers, W.A. Hamilton (Eds.), International Tables for X-ray Crystallography. Kynoch Press, Vol. IV, Birmingham, UK, 1974.
[25] A.L. Spek, Utrecht University,Utrecht, The Netherlands, 2005.
[26] S.V. Krivovichev, Cryst. Rev. 10 (2004) 185–232.
[27] J.V. Smith, Chem. Rev. 88 (1988) 149–182.

[28] J. Yu, K. Sugiyama, K. Hiraga, N. Togashi, O. Terasaki, Y. Tanaka, S. Nakata, S. Qiu, R. Xu, Chem. Mater. 10 (1998) 1208–1211.
[29] J. Yu, R. Xu, Acc. Chem. Res. 36 (2003) 481–490.
[30] P.C. Burns, J.D. Grice, F.C. Hawthorne, Can. Miner. 33 (1995) 1131–1151.
[31] F.C. Hawthorne, S.V. Krivovichev, P.C. Burns, Rev. Miner. Geochem. 40 (2000) 1–112.
[32] F.C. Hawthorne, Miner. Mag. 62 (1998) 141–164.
[33] F.C. Hawthorne, Acta Cryst. A 39 (1983) 724–736.
[34] I.D. Brown, The Chemical Bond in Inorganic Chemistry. The Bond Valence Model, Oxford University Press, Oxford, UK, 2002.
[35] P.C. Burns, M.L. Miller, R.C. Ewing, Can. Miner. 34 (1996) 845–880.
[36] F.C. Hawthorne, Am. Miner. 70 (1985) 455–473.
[37] F.C. Hawthorne, Can. Miner. 24 (1986) 625–642.
[38] F.C. Hawthorne, Acta Cryst. B 50 (1994) 481–510.
[39] N.W. Alcock, M.M. Roberts, Acta Cryst. B 38 (1982) 1805–1806.
[40] A.A. Lychev, L.G. Mashirov, Y.I. Smolin, Y.F. Shepelev, Radiokhimiya 30 (1988) 412–416.
[41] G.H. Swihart, P.K.S. Gupta, E.O. Schlemper, M.E. Back, R.V. Gaines, Am. Miner. 78 (1993) 835–839.
[42] J.C. Taylor, P.W. Wilson, Acta Cryst. B 30 (1974) 169–175.
[43] P.C. Burns, K.A. Hughes, Am. Miner. 88 (2003) 1165–1168.
[44] M.S. Grigor'ev, A.A. Bessonov, N.N. Krot, A.I. Yanovskii, Y.T. Struchkov, Radiokhimiya 35 (1993) 17–23.
[45] M.S. Grigor'ev, A.I. Yanovskii, Y.T. Struchkov, A.A. Bessonov, T.V. Afonas'eva, N.N. Krot, Radiokhimiya 31 (1989) 397–403.
[46] N.N. Krot, I.A. Charushnikova, M.S. Grigor'ev, M. S. In 22emes Journees des Actinides Meribel, France, 1992, p. 35.
[47] M.S. Grigor'ev, I.A. Charushnikova, N.N. Krot, A.I. Yanovskii, Y.T. Struchkov, Radiokhimiya 35 (1993) 388–393.
[48] I.A. Charushnikova, N.N. Krot, Z.A. Starikova, Radiokhimiya 43 (2001) 435.